Investigation of the heliconical smectic $SmC_SP_F^{hel}$ phase in achiral bent-core mesogens derived from 4-cyanoresorcinol

J. K. Vij,[1,*] Yu. P. Panarin,[1,2] S. P. Sreenilayam,[1,†] M. Alaasar,[3,4] and C. Tschierske[3]

[1]*Department of Electronic and Electrical Engineering, Trinity College Dublin, The University of Dublin, Dublin 2, Ireland*

[2]*School of Electronic and Electrical Engineering, Kevin Street Dublin 8, Ireland*

[3]*Institute of Chemistry, Organic Chemistry, Martin-Luther-University Halle-Wittenberg D06120, Germany*

[4]*Department of Chemistry, Cairo University, Giza, Egypt*

(Received 17 December 2018; revised manuscript received 25 February 2019; published 30 April 2019; corrected 9 July 2019)

Two 4-cyanoresorcinol-derived achiral bent-core liquid crystalline materials with terephthalate wings terminated by long alkyl chains C_nH_{2n+1}, $1/n = \mathbf{1/16}$ and $\mathbf{1/18}$, are investigated. Both compounds form a paraelectric smectic phase with uniform (synclinic) molecular tilt in layers of the SmC phase composed of fluctuating polar clusters (polarization randomized SmC_SP_R phase). On cooling, the polar coherence length continuously grows and at the distinct phase transition from SmC_SP_R, a synclinic SmC_SP_F phase is formed. The latter turns into a heliconical phase, formed either spontaneously for $\mathbf{1/16}$ or after application of an ac field for $\mathbf{1/18}$. The helical structure has a helical axis perpendicular to the layer planes and is stable over a relatively broad range of temperatures. The spontaneously helical phase, formed by achiral molecules, is described as $SmC_SP_F^{hel}$ where *S*, P, *F*, and "*hel*" stand for the synclinic, polar, ferroelectric, and helical, respectively. The helical structure is confirmed by measurements of the birefringence in planar-aligned cells as well as by conoscopy in homeotropic-aligned cells with in-plane electric field. The field applied in a plane at right angles to the helix axis leads to the deformed helical ferroelectric mode, and the field dependency of the apparent tilt angle unequivocally confirms that the phase under study is helical. It is concluded that the structure of this helical phase is similar to that of the SmC_α^* phase formed by permanently chiral rodlike mesogens. Due to the achiral nature of the molecules, $SmC_SP_F^{hel}$ can alternatively be considered as $SmCP_\alpha$ phase. Since the helical pitch is approximately the same for both $\mathbf{1/16}$ and $\mathbf{1/18}$, in spite of different molecular lengths and its correspondence of the structure with $SmCP_\alpha$ (like SmC_α^* for chiral molecules) the helical pitch is suggested to be incommensurate with the integral number of the layers. The relationship of this mirror-symmetry-broken polar helical phase with an apolar twist bend smectic phase of mesogenic dimers is also discussed.

DOI: 10.1103/PhysRevMaterials.3.045603

I. INTRODUCTION

Bent-core liquid crystalline compounds having a 4-cyanoresorcinol core and two rodlike terephthalate wings, terminated on both ends by alkyl chains C_nH_{2n+1}, $1/n = \mathbf{1/16}$, and $1/n = \mathbf{1/18}$, exhibit a number of interesting phases. These phases were identified using a combination of techniques that included differential scanning calorimetry, polarizing optical microscopy (POM), and x-ray diffraction. The chemical structure, phase sequence, transition temperatures (T/°C), and the corresponding transition enthalpies (ΔH/kJ mol^{-1}) under cooling are given in Fig. 1 [1,2].

The phases of interest in this paper are the synclinic tilted polar smectic phases (SmC_S) named SmC_SP_F and $SmC_SP_F^{hel}$. $SmC_SP_F^{hel}$ is considered as a heliconically twisted ferroelectric SmC_SP_F phase. It is a stable one for compound $\mathbf{1/16}$, but for compound $\mathbf{1/18}$ its formation appears to be inhibited by a stabilization of the polar SmC_SP_F state by polar surface anchoring. The adjacent phases are SmC_AP_A (anticlinic tilted polar antiferroelectric) on the low-temperature side and a synclinic tilted paraelectric SmC_S phase (SmC_SP_R) on the higher-temperature side. In the latter paraelectric phase, the fluctuating polar clusters have an appreciable coherence length; therefore they can be switched under a strong electric field, but without applied field the polarization is randomized.

The $SmC_SP_F^{hel}$ phase has the potential for applications in devices which can successfully be used in photonics, optical communications, and displays. The devices incorporating these liquid crystalline (LC) materials in their $SmC_SP_F^{hel}$ phase satisfy the characteristics of better alignment, large contrast ratio, and operability under low electric fields [1]. Therefore, a general interest exists in the understanding of the formation of this phase and of formulating molecular design rules for the compounds that exhibit this phase over a wide range of temperatures.

The $SmC_SP_F^{hel}$ phase is obtained on cooling from the SmC_SP_R phase [3]. The latter is considered as a *tilted* analog of the orthogonal polar random smectic phase, $SmAP_R$ [4–6], in which the molecules exhibit no (or randomized) tilt. Although the phase SmC_SP_R has a uniform tilt, coupling between the polar and tilt directions is weak, due to a low potential barrier for the rotation of these weakly bent

*Corresponding author: jvij@tcd.ie

†Present address: Advanced Processing Technology Research Centre, School of Mechanical & Manufacturing Engineering, Dublin City University (DCU), Glasnevin, Dublin-9, Ireland.

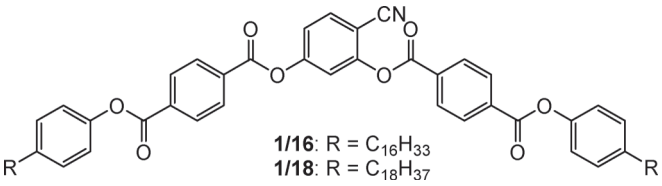

1/16: Iso 162 [-7.9] SmA 125 [-] $SmCP_R$ 110 [-0.8] $SmC_SP_F^{hel}$ 90 [-] SmC_AP_A 77 [-38.8] Cry

1/18: Iso160 [-7.4] SmA 134 [-] SmC_SP_R 111 [-0.9] SmC_SP_F ($SmC_SP_F^{hel}$) 90 [-] SmC_AP_A 76 [53.1] Cry

FIG. 1. Structural formula of the compounds, their phase transitions (T/°C) on cooling, with transition enthalpies given within square brackets [ΔH/kJ mol^{-1}]. For abbreviations, see the list of abbreviations given in the Appendix. In **1/18**, SmC_SP_F or $SmC_SP_F^{hel}$ exists depending on the external conditions. SmC_SP_F is a surface-stabilized state in the absence of the applied field, where $SmC_SP_F^{hel}$ is a uniaxial helical phase structure induced by a pulsed E field and is stable once formed. Here the parentheses do not imply that $SmC_SP_F^{hel}$ is a monotropic phase.

4-cyanoresorcinal-based molecules around their long axes. One of the main reasons is the weaker molecular bend; the angle between the rodlike wings is about 140°, relatively wider compared to a narrower 120° angle of the usual bent-core mesogens. Therefore, its polar directions are randomized either within the same domain or over a combination of domains, macroscopically. The consequence of the random polar directions is the absence of the net spontaneous polarization ($P_S = 0$) in the SmC_SP_R phase, as in the $SmAP_R$ phase [6].

In this paper, we provide additional confirmation of the heliconical structure of the $SmC_SP_F^{hel}$ phase. Results of these investigations will lead to an improved understanding of the origin of the helical structure in LC phases formed by achiral bent-core mesogens. We investigate similarities and differences with the recently reported twist-bend heliconical SmC_{TB} phase formed by achiral bent mesogenic dimers [7]. A comparison of the uniaxial $SmC_SP_F^{hel}$ with the previously known uniaxial SmC_α^* phase formed from chiral rodlike molecules [8] is also made.

II. RESULTS AND DISCUSSION

During the phase transition from SmC_SP_R to SmC_SP_F under cooling, a significant drop in the birefringence of a planar-aligned LC sample is observed. Results are shown in Fig. 2. In Fig. 2(a), a decrease in birefringence at its transition from SmC_SP_R to SmC_SP_F is recorded in the absence of an external electric field. This drop in birefringence can conceivably be due to the formation of a helical structure since the nontwisted SmC_SP_F structure with the same tilt angle will have a higher birefringence. As a consequence the phase is labeled as $SmC_SP_F^{hel}$ (S, P, F, and *hel* stand for the synclinic, polar, ferroelectric, and helical, respectively). The birefringence increases as the helix is gradually unwound by the dc electric field, E. For the compound $1/n = \mathbf{1/18}$ [Fig. 2(b)], formation of the helix is not spontaneous; it is only formed after application of a pulsed electric field E applied across a planar-aligned cell, for the duration in time of as short as ∼10 s, and it is stable after removal of the field. The helix thus formed is unwound by an external dc field, E, and returns back to the initial helical state immediately on removal of the applied dc field. Hence, after the first treatment of SmC_SP_F by an ac field, the phase structure can reversibly be switched between the helical and unwound states by removal and application of the external dc field, respectively. For **1/16** this on-off switching of the helical superstructure does not require the initial ac field treatment, meaning that there is a stronger driving force for the helix formation of **1/16**. The magnitude of the helical pitch has previously been determined by immersing the LC filled cell (after ac treatment in case of **1/18**) into a Dewar filled with liquid nitrogen. The LC cell was force opened and the helical structure frozen in its glassy state was scanned using a high-resolution atomic force microscope (AFM) at room temperature. The helical pitch was measured as 14 nm for **1/18** and 15 nm for **1/16** [1]. The helical pitch values are valid for the temperatures from where the supercooling of the sample was initiated.

From results of the birefringence, the heliconical angle θ_0 is calculated using the formula [9]

$$\Delta n\,(\theta_0) = \frac{\Delta n_0}{2}\,(3\cos^2\theta_0 - 1). \qquad (1)$$

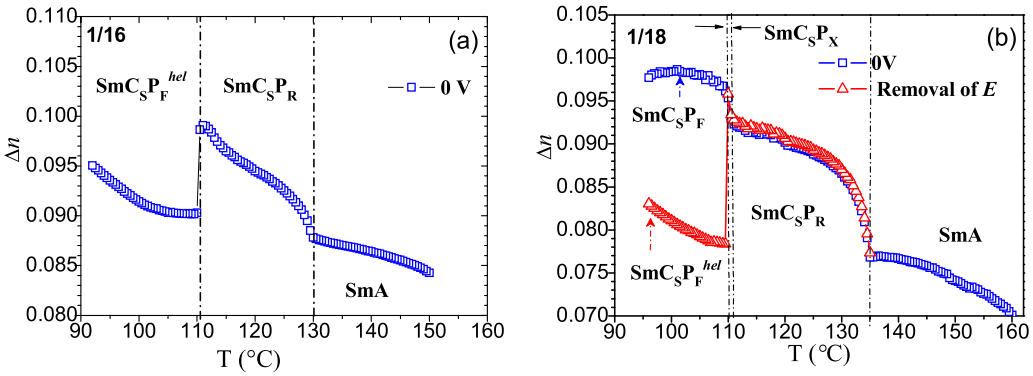

FIG. 2. (a), (b) Plots of the birefringence Δn as a function of temperature for **1/16** and **1/18** filled in planar-aligned cells of cell thickness 9 μm. In (a) the drop in Δn at the SmC_SP_R to SmC_SP_F phase-transition temperature is instantaneous for $E = 0$. In (b) the drop in Δn occurs on the removal of the external field. In each case the optical retardation ($\Delta n \cdot d$) is measured and the birefringence is calculated by dividing the retardation by the cell thickness. For an explanation of SmC_SP_X phase, see Ref. [2].

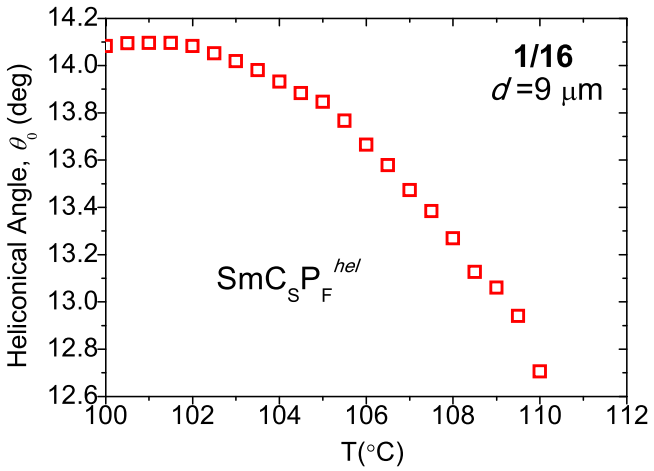

FIG. 3. Heliconical angle θ_0 (the angle between the local director that draws an oblique helicoid and the helical axis) calculated from measurements of the birefringence as a function of temperature.

The heliconical angle is defined as the angle between the local director that draws an oblique helicoid and the optical (or helical) axis. Δn_0 is the birefringence of the unwound synclinic structure and is dependent on temperature. This is extrapolated to a temperature where Δn is measured; θ_0 is the heliconical angle for this particular temperature. Results of θ_0 for **1/16** are shown in Fig. 3. It is interesting to note that θ_0 increases continuously with a reduction in temperature similar to that of the $N_{\rm TB}$ phase [9–12], with the proviso that θ_0 lies in a narrow range of values, from 12.6° to 14.1° in this case. Normally a large electric field is needed to unwind the helix in $N_{\rm TB}$ phase [13,14]. However, an unwinding of the helical structure of $1/n$ is brought about by a moderately weak field of $1\,{\rm V}/\mu{\rm m}$. It is natural to expect that such a heliconical structure would lead to a deformed helical ferroelectric (DHF) mode on the application of dc external field. The switching time of the DHF mode is measured to be in the range 30-40 μs [15]. The speed of switching is faster by a factor of 100 compared to conventional FLCs composed of the rodlike chiral molecules in DHF mode. A faster switching time is a consequence of a shorter helical pitch in SmC$_S$P$_F^{hel}$ of **1/16** and **1/18** by at least two orders of magnitude than for the conventional ferroelectric liquid crystals (FLCs). The pitch in the latter class of materials is of the order of a few μm [16,17].

We offer additional evidence for the formation of helix in $1/n = \mathbf{1/16}$ using the technique of conoscopy, where images of the refractive indices ellipsoid under field can lead to a procedure of finding refractive indices in the three orthogonal directions. These are used to determine the biaxiality and the birefringence of the system. We use an optical polarizing microscope (Olympus BX-52) [18] equipped with a port for the Bertrand lens. This port is present in between the objective and the ocular. Two separate lenses, each with a large numerical aperture (NA) for the objective and the condenser, are used. These are needed to have a wider observable field of view of refractive indices ellipsoid as well as of requiring a long working distance for the hot stage used for controlling the temperature of the LC cell. The lens for the objective used is Olympus, LM Plan FI; 50, 0.5 NA and for the condenser the lens used is Instech Co.; 0.65 NA. The LC cell used has 6.5-μm cell spacing in between the two substrates. These are coated with a homeotropic aligning agent (AL60702, JSR Korea). The conoscopic images of a homeotropic-aligned cell are recorded by varying the in-plane electric field E. The field is increased in steps of the field varying up to $6\,{\rm V}/\mu{\rm m}$. Results of the experiment are given in Fig. 4. For $E = 0$, the observed conoscopic image is uniaxial; the resulting structure becomes increasingly biaxial as the in-plane electric field is increased. We find that the biaxiality of the smectic phase is saturated for an electric field strength of $5.25\,{\rm V}/\mu{\rm m}$. On the removal of an external field, the structure returns back to being uniaxial again instantaneously [from Figs. 4(e) to 4(a)].

III. TEXTURES OF A PLANAR-ALIGNED THIN CELL FOR THE COMPOUND $1/n = 1/16$ AND THEIR EXPLANATIONS

Textures for a planar-aligned cell of spacing 2 μm are shown in Figs. 5(a) to 5(d).

It is interesting to note that in a planar-aligned cell of thickness 2 μm, both bright and dark domains are observed for the cell in SmC$_S$P$_R$ phase of **1/18**, textures of which are shown in Figs. 5(a) and 5(b). In this phase, the tilt angle for the two domains is the same but the molecules in the neighboring domains are tilted to the left and to the right of the layer normal L. The directions of stripes coincide with the rubbing direction R as shown in Fig. 6. The polar directions in SmC$_S$P$_R$ are random [3,19]. On lowering the temperature of the cell, the sample enters in its SmC$_S$P$_F$ phase where the helical structure SmC$_S$P$_F^{hel}$, as indicated above, is spontaneously formed. In this phase, the texture is shown in Fig. 5(c) where the dark and bright stripes parallel to R are observed; here the domain boundaries appear normal to R. Such a texture continues to be displayed down to lower temperatures, Fig. 5(d), except that the brightness of texture suddenly drops to a lower level. In addition to the display of the stripes parallel to R, the stripes normal to R are also observed. The latter arise from the instability in some of the elastic constants of the LC sample reducing to very small values; the observed phenomenon is similar to that of the $N_{\rm TB}$ phase [20].

One naturally asks an important pertinent question as to why the SmC$_S$P$_F$ phase emerges at a lower temperature when the free energy of the SmC$_S$P$_A$ is lower than that of SmC$_S$P$_F$. The most likely answer is that the SmC$_S$P$_F$ phase is macroscopically chiral and its chirality synchronizes with the transient chirality of the same handedness. Why is the helix formed? This is the result of a synchronization of the helical sense with that of the transient molecular chirality, which results in forming the helix of a particular sense [21]. The helix is energetically favored as it results in a denser packing of the molecules than those for a disordered structure in the absence of the helix. The helix once formed is stabilized as the structure escapes from a large spontaneous polarization of the domain.

IV. THE SmC$_S$P$_F^{hel}$ PHASE BY DIELECTRIC SPECTROSCOPY AND POLARIZATION

The dielectric spectroscopic measurements clearly establish that the phase at a temperature of 106 °C, for **1/16**, is ferroelectric. The dielectric amplitude increases significantly

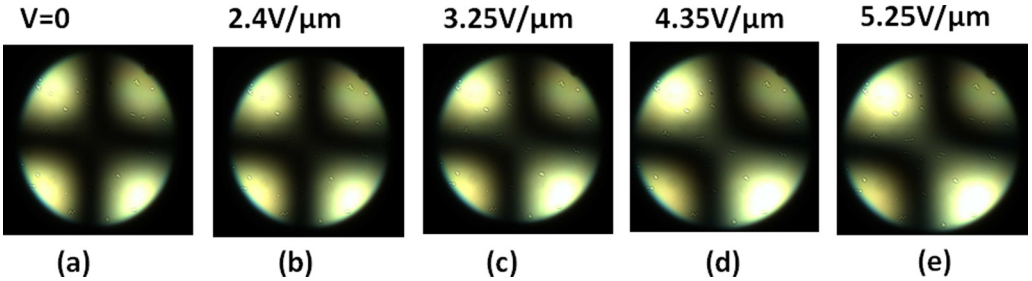

FIG. 4. (a)–(e) Conoscopic images of a homeotropic-aligned cell of **1/16**; the cell thickness is 6.5 μm. The two lenses, each with a large numerical aperture, are used for the objective and the condenser. The lens for the objective is Olympus, LM Plan FI; 50×, 0.5 NA and for the condenser it is 20×, 0.4 (Instech, 0.65 NA). The in-plane electric field of a square wave signal of frequency, $f = 110$ Hz, is applied across the in-plane electrodes of a homeotropic-aligned cell. The cell is kept at an angle of 45° to the polarizer/analyzer directions.

on cooling from the SmC_SP_R to SmC_SP_F. It is followed by a sudden decrease in its dielectric amplitude due to having the helical structure formed (see Fig. 9a in Ref. [2]). The helical phase gives rise to a small value of the apparent tilt angle θ_{app} on the application of a weak probe field. This is indicative of a large amplitude of the soft-mode fluctuations seen in Figs. 9(a) and 9(b) of Ref. [2] (a large decrease in the frequency is observed as the paraelectric-to-ferroelectric transition is approached). On its entry under cooling from SmC_SP_R to the temperature range of 110 to 90 °C corresponding to SmC_SP_F, the initial biaxial structure seen in the conoscopic images suddenly transforms to a uniaxial one. This is naturally a consequence of a spontaneous formation of the helical structure in a cell and for this reason the phase is denoted as $SmC_SP_F^{hel}$. An increase in the field gradually unwinds the helix; consequently, the ensuing phase becomes increasingly biaxial as the helical structure is distorted by increasing E, shown above in Fig. 4. As stated already, a large field is required for producing a distortion in the helical structure of N_{TB} [13,14]. Nevertheless, the distortions in the helical structure of a bent-core system that arise from applying relatively low fields are an exception, which usually is due to a large negative dielectric anisotropy of this LC material in its N_{TB} phase [12]. The observation of $SmC_SP_F^{hel}$ is reminiscent of a short pitch exhibited by a uniaxial SmC_α^* phase formed by chiral rod-shaped molecules [8]. Since we are dealing with the polar bent-core achiral systems here and the bent-core angle is ∼140°, the phase is justifiably labeled as $SmCP_\alpha$ [19]. There

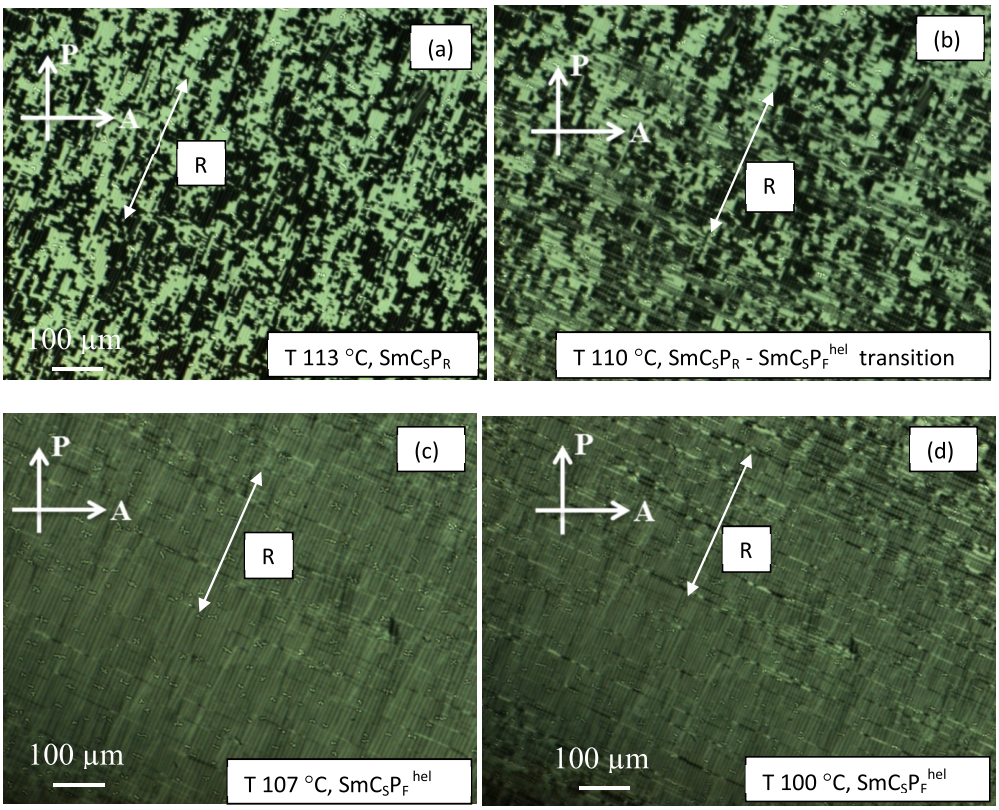

FIG. 5. (a)–(d) Textures of SmC_SP_R and SmC_SP_F phases of **1/18**, planar-aligned cell of cell thickness 2 μm. The birefringence for $SmC_SP_F^{hel}$ in (c) and (d) at temperatures of 107 and 100 °C are observed to be lower than for the SmC_SP_R phase. The stripes parallel to the rubbing direction, R, are seen in (c) and the stripes both parallel and perpendicular to R are seen in (d).

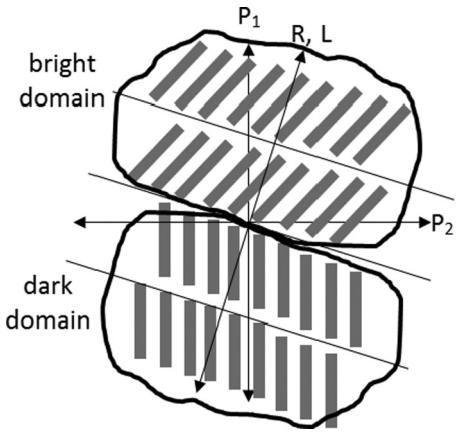

FIG. 6. Schematics of bent-core molecules (shown here as rod-like) arranged in the SmC_SP_R phase. The molecules display a uniform tilt angle, leading to $(-)SmC_SP_F$ and $(+)$ SmC_SP_F domains of opposite chiralities. The minus (plus) signs in the parentheses indicate negative and positive layer chiralities, respectively.

does exist a compelling physical reason too for the formation of a helical structure such as an escape from the large Ps that arises in turn from molecular chirality and a large dipole moment. According to a simple phenomenological theory of Pikin and Indenbom [22], the helical pitch in the SmC^* phase is expressed by the wave vector q,

$$q = \frac{2\pi}{p_0} = \frac{\Lambda + \mu P_S/\theta}{K}. \tag{2}$$

p_0 is the pitch of the undisturbed helix, μ is the flexoelectric coefficient, P_S is the spontaneous polarization, θ is the molecular tilt angle, K is the effective elastic constant, and Λ is the Lifshitz invariant. The latter is responsible for the formation of helix of a given handedness and this seemingly arises from molecular chirality. An existence of the nonzero polarization shortens the helical pitch, while the sense of helix is determined by the sign of Λ. For achiral molecules, $\Lambda = 0$, pitch p_0 of the helical structure is given by

$$p_0 = 2\pi K\theta/\mu P_S, \tag{3}$$

For large values of $P_S = 400$ nC/cm^2 and for large μ/θ, and relatively small effective elastic constant K of the LC, the helical pitch is justifiably low, $p_0 \sim 15$ nm. In other words, formation of the helix reduces the electrostatic energy and increases the elastic energy; magnitude of the pitch is determined as a consequence of the balance in between these two competing forms of energy. A synchronization of the transient handedness of chirality of the conformers with the helical sense leads to spontaneous symmetry breaking of achirality, and therefore to the sign of Λ. Hence, the helical structure once formed stabilizes one of the two possible chiral conformations that arise from the matching of diastereomeric coupling with the "transient chirality" of molecular conformations. For $\Lambda \neq 0$, we have either $\Lambda = +1$ or -1 depending on the sense of the helix. A finite value of the parameter Λ additionally stabilizes the helical structure with a shorter helical pitch, as seen from Eq. (2).

V. THE DEFORMED HELICAL FERROELECTRIC EFFECT

The DHF effect was discovered initially for FLCs by Beresnev *et al.* [23]. The DHF mode deals with an initial distortion of the helix brought by the dc field $E < E_{th}$, where E_{th} is the threshold electric field. Above the field E_{th}, a nonlinear increase in the induced tilt angle is observed with the field, see Fig. 7(b). For achiral systems, the symmetry breaking leads to left- and right-handed helical structures, albeit these might exist spatially over different parts of LC cell [1,2].

The transmitted light T passing through a planar-aligned LC cell under crossed polarizers is given by the equation

$$T = A \sin^2 2(\alpha' \pm \beta') \sin^2\left(\frac{\pi \Delta n d}{\lambda}\right). \tag{4}$$

Here α' is the angle between the polarizer P and the optical axis; β' is the apparent tilt angle θ_{app}. Δn is the birefringence, d is the cell thickness, and λ is the wavelength of the transmitted light. T is the transmitted light through the cell under crossed polarizers of a POM with the retardation $\Delta n \cdot d$. The transmitted intensity T is recorded and the birefringence Δn calculated. On assuming that a change in the birefringence Δn is not significantly dependent on E, the term $\sin^2\left(\frac{\pi \Delta n d}{\lambda}\right)$ approximates to a numerical constant for small values of E. The phenomenon can be observed in two configurations of the cell. In configuration 1, rubbing direction (R) is fixed along the polarizer, i.e., $\alpha' = 0$; $\beta' = 0$ for $E = 0$. The layer normal L is along $\boldsymbol{n}$. In this configuration, the helix is distorted by E applied in a plane normal to the helical axis; the apparent tilt angle $\theta_{app} = \beta'$ is linearly related to E as shown in Fig. 7(b) (third on the right). The initial state is dark, which turns bright for both polarities of E. This therefore is a nonlinear mode in the transmitted intensity, T. In configuration 2, α' is fixed at an angle of 22.5° to the polarizer direction; the brightness of the initial state is intermediate between those of the dark and bright states. This mode of T is therefore linear within the limits of a small change in θ_{app} with E. and the two polarities of E with $\alpha' = 22.5°$ cause the transmitted signal to be darker or brighter depending on the sign of E. A large field E gives rise to a complete unwinding of the helix and consequently leads to a complete electro-optical (EO) switching.

An application of E leads initially to a linear followed by nonlinear increase of T with E and then it results in a "full switching" as a result of "a complete helical unwinding" brought about by E. This gives rise to an observation of the so-called V-shaped switching. Nevertheless, for higher temperatures [95 and 105 °C here] and for higher fields, the amplitude of the EO response expressed by T decreases by increasing E; this is shown in Fig. 8. This is suggested to be due to an emergence of the multiple domains of a tilted smectic phase in the field of view of the polarizing optical microscope as being suggested below. During the linear operational regime of DHF mode, where θ_{app} is proportional to E (see Fig. 7(B)), switching time is independent of E. A further increase in E results in a sudden increase in the effective value of the pitch, when the helix is finally unwound by large E. An ultimate saturation in the magnitude of the tilt angle with E is reached and consequently P_S is saturated with E (Fig. 8, $T = 80$ °C).

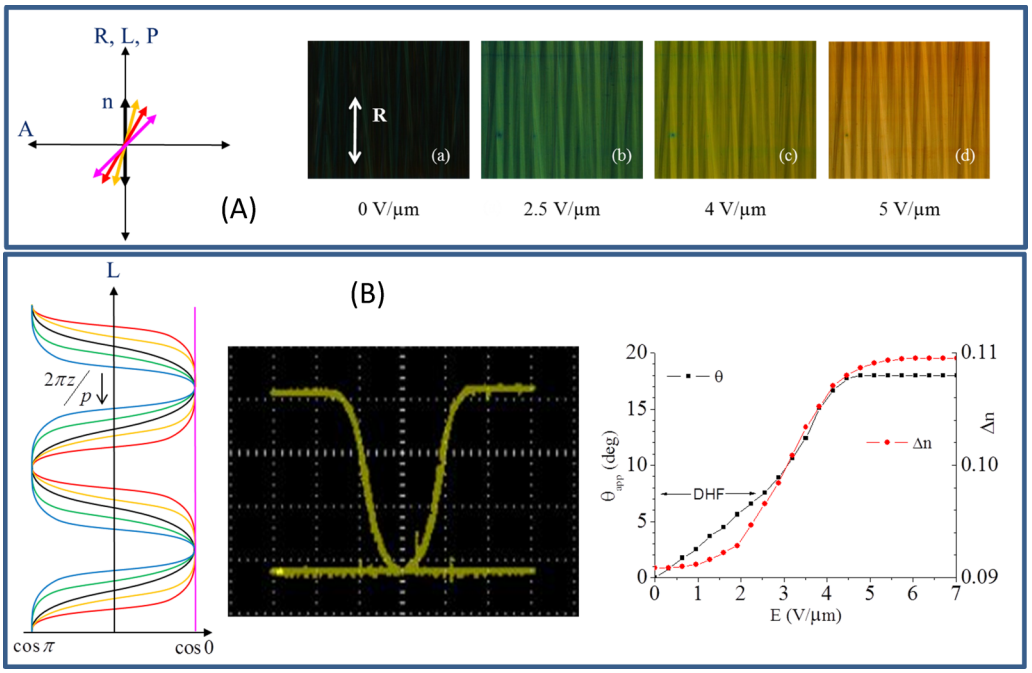

FIG. 7. (A) In cell configuration 1, the rubbing direction (R), layer normal (L), and the director $\boldsymbol{n}$ coincide with each other. R, L, and $\boldsymbol{n}$ are shown to lie along the direction of the polarizer. An increase in the electric field (E) applied in a plane at right angles to the helical axis distorts the helical structure. $\boldsymbol{n}$ is rotated by E from its position along L, accompanied by the helical distortion (shown by arrows of different colors; see A and B both extreme left). When an applied electric field is large enough, helix eventually is completely unwound (see B), leading to $\varphi = n \cdot \pi$, where n is an integer including zero. φ is the azimuthal angle between the $\boldsymbol{c}$ direction (the projection of the director onto the smectic layer) and the reference direction on the substrate. The V-shaped switching (see B middle) is a result of the helical unwinding brought about by E and its shape results from a plot of T vs E. In (B) extreme right, the apparent tilt angle and the birefringence are plotted as a function of E, where the DHF mode is a linear variation of apparent tilt angle with E.

Nevertheless, for a higher temperature of 95 °C, the EO response expressed in terms of T reaches maximal amplitude for $E \sim 3\,\mathrm{V}/\mu\mathrm{m}$ and then it starts to decrease for $E \sim 5\,\mathrm{V}/\mu\mathrm{m}$ instead of staying on a plateau or slightly increasing with E. The POM shows that the texture splits into two different domains: the EO switchable and the EO nonswitchable. The size of nonswitchable domain increases with an increase in E. On the other hand the electro-optic response (or Ps) does not show any drop in its value with the field. This effect is even more pronounced for a temperature of 105 °C where the texture becomes completely nonswitchable for $E \sim 6\,\mathrm{V}/\mu\mathrm{m}$ and higher. Such a phenomenon is satisfactorily explained by a model given by Nakata *et al.* [24]. At the outset, the model considers two competing dynamical mechanisms, shown in Fig. 9. One of the two mechanisms involves "chiral flipping" without the electro-optical switching occurring. This mechanism involves the rotation of the dipole moment (arising from "a combination of the layer chirality and a large transverse dipole moment") around the long molecular axis and accounts for Ps with the field. The second dynamical process relates to the electro-optical switching of the optical axis (e.g., its rotation of the optical axis by an angle φ around the cone). Which of the two processes is dominant at a particular temperature and the applied field depends on the relative values of the energy barriers for these two mechanisms and the strength of the electric field.

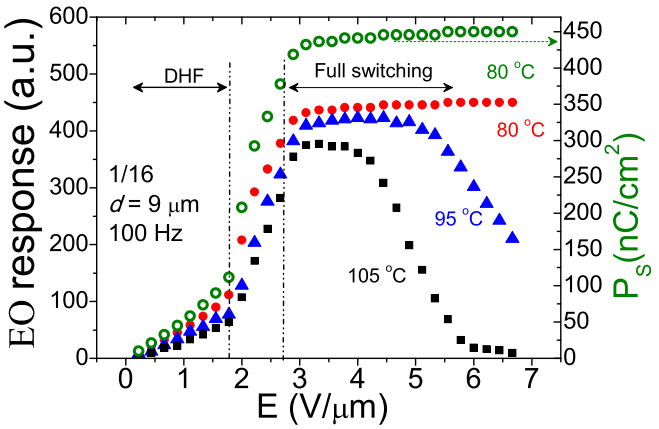

FIG. 8. Amplitude of the EO response in **1/16** as a function of E plotted for different temperatures in the $\mathrm{SmC}_S\mathrm{P}_F^{hel}$ phase. The DHF effect relates to an initial linear distortion of the helix by E rising to $1.8\,\mathrm{V}/\mu\mathrm{m}$, where the response in T is linear with E and results in $P_S \approx 150\ \mathrm{nC/cm^2}$. P_S is shown by the green curve; the other curves correspond to transmittance through the cell.

The solution of the model is given by the two related differential equations:

$$\frac{d\beta}{dt} = \frac{P_0 E(\sin\beta\,\cos\varphi + \sin\varphi\cos\beta\cos\theta) - \left(\frac{dU_b}{d\beta}\right)}{\eta_\beta} - \frac{d\varphi}{dt}\cos\theta, \tag{5}$$

$$\frac{d\varphi}{dt} = \frac{P_0 E \sin\varphi\cos\beta\,\sin^2\theta + \left(\frac{dU_b}{d\beta}\right)\cos\theta}{\eta_\varphi - \eta_\beta\,\cos^2\theta}. \tag{6}$$

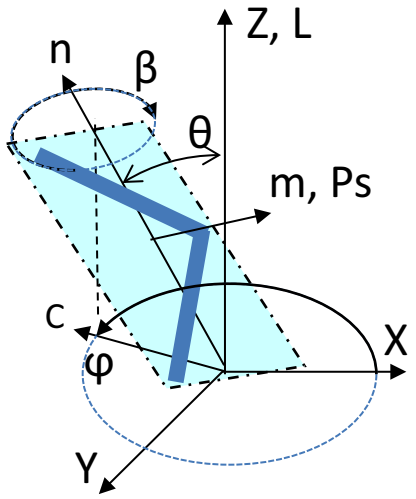

FIG. 9. Laboratory coordinate system (X, Y, Z) and the tilted SmC-like bent-core phase, where θ is molecular tilt angle that $\boldsymbol{n}$ makes with $\boldsymbol{L}$, $\boldsymbol{L}$ is smectic layer normal, which lies along the direction Z. X-Y is the smectic layer plane, $\boldsymbol{n}$ is a molecular main axis/director, $\boldsymbol{m}$ is short axis, $\boldsymbol{C}$ is the $\boldsymbol{c}$ director defined as the projection of $\boldsymbol{n}$ on the smectic layer plane, Ps is the in-layer spontaneous polarization. There are two possible rotational mechanisms: (i) the rotation of the molecular long axis on a cone around the smectic layer normal (measured by an angle φ that the $\boldsymbol{c}$ director makes with respect to the X axis) and (ii) rotation of the short axis around the long molecular axis measured by an angle β that the short axis makes with respect to the reference direction.

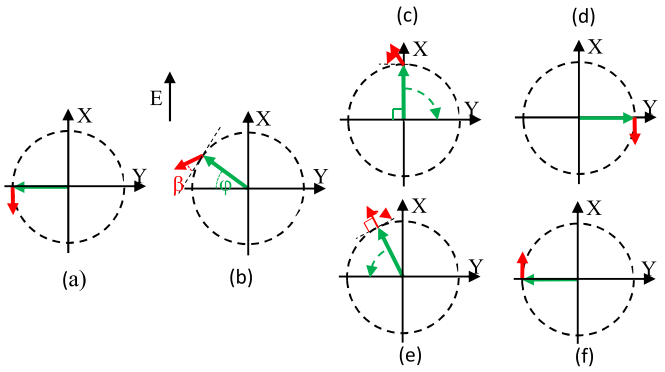

FIG. 10. X-Y plane is the smectic layer plane. Y-Z is the plane of the substrate. Z is normal to the plane of the paper. Z is the rubbing direction shown parallel to the layer normal. X is the field direction. The green arrow describes rotation of the optical axis around the cone by an angle φ (electro-optical switching) whereas the red arrow, the direction normal to the molecule, describes rotation by β (corresponding to the chiral flipping) in SmC_SP_F phase. (a) Initial state prior to electric-field reversal, defined by $\beta = 0^\circ$ and $\varphi = 0^\circ$, (b) initial dynamics after the field reversal, $0^\circ < \beta < 90^\circ$ and $0^\circ < \varphi < 90^\circ$, (c) critical state for the EO switching, $0^\circ < \beta < 90^\circ$ and $\varphi = 90^\circ$ is reached, (d) the final switching state $\beta = 0^\circ$ and $\varphi = 180^\circ$, (e) critical state for the chiral flipping, $0^\circ < \varphi < 90^\circ$ and $\beta = 90^\circ$, (f) final chiral flipping state $\varphi = 0^\circ$ and $\beta = 180^\circ$.

Equation (5) describes the rotational dynamics by angle β (the rotation of the short axis around the long molecular axis), whereas Eq. (6) expresses the rotational dynamics of the director/optical axis through an angle φ around the molecular cone. The first mode involves Ps whereas the latter accounts for the EO switching as well as of Ps. θ is the tilt angle of a tilted smectic phase. In the above equations, U_b is the internal energy barrier dependent on the angle β and is given by

$$U_b(\beta) = U_{\max}(\sin^2\beta + k\cos\beta). \tag{7}$$

The first term in Eq. (7) involving $\sin^2\beta$ is valid for $U_{\max} > 0$. This relates to the spontaneous symmetry breaking, while it gives to chiral degenerated states (the case of SmCP phase of achiral molecules), whereas the second term, $k \neq 0$, accounts for the chiral molecules. We consider later that $U_{\max}$ depends on temperature as well.

The experimental results show that for $E < E_C$, the switching occurs by rotation of the optical axis around the cone φ, whereas for $E > E_C$, the LC sample shows chiral flipping through the molecular rotation of the short axis by an angle β around its long molecular axis. According to this model [24] the critical field E_C depends linearly on the energy barrier $U_{\max}$. On a reversal of E, the dynamics occurs simultaneously by both β and φ, see Fig. 10. The final outcome however depends on which of the two angles, β or φ, reaches the critical value of 90° first. The angle β or φ which reaches 90° first continues to increase and finally reaches 180° (complete switching), while the second of the two returns back to its initial 0° position with reverse dynamics occurring. According to this model, the optical switching occurs around the cone for a lower field of E, while the chirality flipping by angle β is the most preferred outcome for higher values of E.

This model, however, does not explicitly explain the observed temperature dependence of the critical field. This is explained by assuming that the energy barrier $U_{\max}$ depends on the molecular tilt angle θ, $U_{\max} = U_0 \sin^2\theta$, where θ is dependent on temperature and U_0 is a constant. For higher temperatures θ is low and consequently $U_{\max}$ is also low. Hence in this case, the chirality flipping is the predominant outcome compared to optical switching occurring around the cone.

The model of Nakata *et al.* [24] is thus able to explain the EO response, expressed in terms of T, as a function of both temperature and the field E in the SmC_SP_F phase.

VI. THE PROPOSED MODEL OF THE HELICAL SMECTIC PHASE $SmC_SP_F^{hel}$

We obtain much evidence for the helical structure in SmC_SP_F phase. These include measurements of the birefringence, the recording and the analysis of the conoscopic images as a function of the in-plane field E applied in a homeotropic-aligned cell, measuring the helical pitch by AFM, the observation of the DHF mode in planar-aligned cell with the field applied and analysis of the results from dielectric spectroscopy. These results have convincingly proven that helical structure exists in the $SmC_SP_F^{hel}$ with the proviso that the helical pitch is short and is of nanometer dimensions. Based on these results, the model proposed for the helical phase of compounds **1/16** and **1/18** is that of $SmCP_\alpha$ phase with a helical pitch of ~15 nm. The proposed model is a tilted version of the $SmAP_\alpha$ phase [6,26]. The model also fits in with the results obtained for both heating and cooling cycles

of a similar compound that has the same core and the same wings, except the wings are terminated by two long alkoxy chains, $C_{14}H_{29}O$ [19]. Here $SmCP_\alpha$ phase is found to coexist with a polarization-modulated smectic phase (designated M1) which under some boundary conditions becomes the more stable of the two phases [19]. Probably the effective molecular conformational helicity is weaker for alkyloxy-substituted compound due to slightly changed bond angles and different heights of the rotational barrier.

In the proposed model, the tilt angle of bent-core molecules in a tilted phase is finite but is dependent on temperature. Nevertheless, the tilt angle in $SmC_SP_F^{hel}$ phase of these compounds stays low over a broad range of temperatures. The tilt angle is of the same order of magnitude as the heliconical angle, which is $\sim 15^\circ$ or less. The latter is calculated from the measurements of the birefringence plotted in Fig. 3. An application of a weak field $E < 0.1\,\mathrm{V}/\mu\mathrm{m}$ applied along the smectic layer, in a plane at right angles to the helical axis, leads to a large polar response. This is evidenced by a large dielectric relaxation strength plotted in Figs. 9(a) and 9(b) in Ref. [2]. If this phase were to be a layered SmC_{TB} [7] but having similar characteristics as N_{TB} except with the addition of smectic layers, the resulting polar response in that case must have been weak in contrast to strong observed experimentally with a large dielectric strength in this case. The authors of Ref. [7] state that the polar response is absent. This would have also required a large field strength for introducing the field-induced distortions in the helical structure. The question arises as to what is the difference between the $SmCP_\alpha$ and SmC_{TB} phases. It has already been pointed out that SmC_{TB} is different from $SmCP_\alpha$ phase as the measurable polar order could be absent in the former [7]. It can therefore be speculated that helicity in SmC_{TB} phase is driven mainly by vanishingly small bend elastic constant of the dimeric compound, whereas for the $SmCP_\alpha$ an escape from the uniform polar structure is important for a stabilization of the helical state. Chiral rodlike liquid crystalline molecules form a uniaxial heliconical SmC^*_α phase with a short pitch, formation of which normally requires a large enantiomeric purity of the compound, but also the tilt angle must be low, which is normally the case only for a narrow range of temperatures in between the SmA^* and SmC^* phases, i.e., SmC^*_α exists only when the interlayer correlations among the adjacent layers are weak and the tilt angle is low. The temperature range of SmC^*_α phase is therefore extremely narrow [8] as the tilt angle needs to be as low as 8° or less. This is normally valid for a limited range of temperatures. In the case investigated here, the helix is also formed when the apparent tilt angle is low [1]. The difference here is that the tilt angle does stay low over a broader range of temperatures; the heliconical structure can thus exist over a broader range of temperatures. In contrast to SmC^*_α, $SmCP_\alpha$ phase is formed by achiral molecules where spontaneous symmetry breaking occurs. These molecules undergo transient chiral conformation and chirality synchronization [21] and for these reasons they contribute to the formation of a helical structure. The helical pitch in terms of a number of layers is incommensurate with an integral multiple of the layer thickness as was proposed for $SmAP_\alpha$ [6,25] phase in line with SmC^*_α phase. This is also suggested to be the case for $SmCP_\alpha$ ($SmC_SP_F^{hel}$) phase as shown in Figs. 11(a) and 11(b).

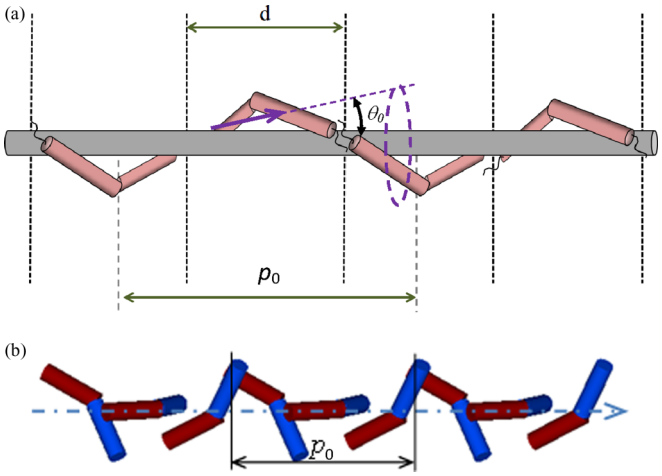

FIG. 11. (a), (b) Model of the $SmC_SP_F^{hel}$ interpreted as that of $SmCP_\alpha$ phase. The director draws an oblique helicoid with an oblique helicoidal angle, θ_0. However the molecules are tilted and twisted. The helical pitch p_o in terms of a number of smectic layers is incommensurate with an integer (the integral number of layers as in SmC^*_α). The helical pitch shown is $\geqslant 2$ times the thickness of a smectic layer, d. Computer-generated image where bent-core molecules appear to form a helical phase. In Fig. 11(b), the bent-core molecules in adjacent layers are twisted by an angle of 110° whereas the bent-core angle $= 140^\circ$. Molecules are tilted by an angle $\ll 90^\circ$ with respect to the helical axis.

VII. HELICAL PITCH OF SmC^*_α PHASE AND ITS CORRESPONDENCE WITH $SmCP_\alpha$ PHASE

SmC^*_α is a uniaxial phase; its helical pitch is known to lie on a nanometer scale. It borders orthogonal smectic A phase on its low-temperature side and SmC^* on its high-temperature side. SmC^*_α is formed only when the tilt angle is 8° or less. In this particular case, the tilt angle found from x rays is vanishingly small and the optical tilt angle is of the order of 5-8° [1]. The theory of Emelyanenko and Osipov [26] can therefore be used to interpret the results of the helical structure. The salient features of the theory include (1) an incorporation of the discrete flexoelectric effect of the adjacent neighboring layers and (2) the use of effective long-range interlayer interactions that arise from a minimization of the polarization-dependent part of the free energy. The equation for the polarization obtained from it is substituted back into the expression for the free energy. The questions arise as to why is the helical pitch of SmC^*_α in terms of a number of layers, commensurate or incommensurate, and why it is of the nanoscale level. The bent-core dimeric molecules separated by an appropriate spacer will have a predominantly large flexoelectric effect [27]. This effect is likely to be of much greater importance than for the rodlike counterparts. Hence the theory in principle should be applicable to the bent-core liquid crystalline systems in the tilted smectic phases that exist in chiral domains formed from the symmetry breaking of achirality.

According to the Emelyanenko-Osipov theory [26] the polarization-dependent part ΔF_i of the total free energy F_i is given by

$$\Delta F_i = \frac{1}{2\chi}\left[\boldsymbol{P}_i^2 + g(\boldsymbol{P}_i \cdot \boldsymbol{P}_{i+1} + \boldsymbol{P}_i \cdot \boldsymbol{P}_{i-1})\right] + \boldsymbol{P}_i \cdot \boldsymbol{M}_i, \quad (8)$$

where $\boldsymbol{P}_i$ is the polarization of the ith layer and the parameter vector $\boldsymbol{M}_i$ is given by

$$\boldsymbol{M}_i \equiv c_p \cos\theta[\boldsymbol{n}_i \times \boldsymbol{k}] + c_f \cos\theta\, \Delta\boldsymbol{n}_{i\pm1}. \tag{9}$$

c_p and c_f in Eq. (9) are, respectively, the piezoelectric and flexoelectric coefficients that contribute to the polarization; in Eq. (8) g is a dimensionless parameter which characterizes the relative strength of coupling. $\boldsymbol{M}_i$ is the order parameter of the ith layer. The inherent assumption here is that the polarization is parallel to the smectic layer itself. This is indeed the case for the bent-core systems in both orthogonal and tilted smectic phases. The nematic director in the $(i+1)$th layer is given by $\Delta\boldsymbol{n}_{i\pm1} = \boldsymbol{n}_{i+1} - \boldsymbol{n}_{i-1}$. On minimizing the entire polarization-dependent free energy expression obtained by summing Eq. (8) over all layers that involve P_i, with respect to P_i, we obtain

$$\boldsymbol{P}_i + g(\boldsymbol{P}_{i-1} + \boldsymbol{P}_{i+1}) = -\chi \boldsymbol{M}_i. \tag{10}$$

It needs to be noted that three adjacent layers actually do involve P_i. On substituting Eq. (10) back into Eq. (8) we obtain

$$\Delta F_i = \tfrac{1}{2}\boldsymbol{P_i} \cdot \boldsymbol{M}_i. \tag{11}$$

This way we can effectively account for the long-range interlayer interactions of layers; the dielectric susceptibility χ and the position correlation factor g are both assumed to be scalar constants to a first approximation. Since the microscopic short-pitch helical structure numerically emerges around the frustration point between the SmA, SmC$^*_\alpha$, and SmC$^*_A$ (SmCP$_A$ phase here instead of SmC$^*_\alpha$) [28–30], we can easily obtain a relationship between $\boldsymbol{P}_i$ and $\boldsymbol{M}_i$ in SmC$^*_\alpha$ phase as follows:

$$\boldsymbol{P_i} = -\frac{\chi}{1 + 2g\cos\Delta\varphi}\boldsymbol{M}_i, \tag{12}$$

where $\Delta\varphi = \varphi_{i+1} - \varphi_i$ is the $\boldsymbol{c}$-director twist-angle difference in between the adjacent layers. On substituting Eq. (12) back into Eq. (8) and by introducing coordinates for vector $\boldsymbol{n}_i$ in terms of the orthogonal unit vectors $\boldsymbol{x}$ and $\boldsymbol{y}$ of the smectic layer plane

$$\boldsymbol{n}_i = \sin\theta(\boldsymbol{x}\cos\varphi_i + \boldsymbol{y}\sin\varphi_i) + \boldsymbol{k}\cos\theta, \tag{13}$$

the polarization-dependent part of the free energy in SmC$^*_\alpha$ per unit smectic layer is given as

$$\Delta F_i = -\frac{\chi}{2(1 + 2g\cos\Delta\varphi)}\sin^2\theta \times \left(c_p^2 + 4c_f^2\sin^2\Delta\varphi - 4c_p c_f \sin\Delta\varphi\right). \tag{14}$$

The pitch of the helix in SmC$^*_\alpha$ and of SmCP$_\alpha$ in this case can be determined by using $p_0 = \frac{2\pi}{\Delta\varphi}$, where the free energy found from the sum of Eq. (14) and Eq. (18) given in Ref. [28] is minimized. Using numerical calculations, we find $\Delta\varphi$ for which the free energy is minimized. The difference angle $\Delta\varphi$ depends only on the physical constants of the system and not on the discrete number of layers. The helical pitch in terms of the number of layers in general may thus be incommensurate with an integral number of layers [28,30,31]. Values of the helical pitch can be calculated numerically by assuming values of the various constants.

VIII. CONCLUSIONS

The existence of a helical structure is confirmed in the synclinic ferroelectric phases of compounds **1/16** and **1/18** formed at the transition from paraelectric to polar smectic phases. For **1/16** helical formation is spontaneous whereas for **1/18** it requires a prior ac-field treatment. The helical structure is confirmed to exist from results of the birefringence measured for planar-aligned cells and conoscopy carried out on homeotropic aligned cells with an in-plane electric field applied. An electric field applied at right angles to the helical axis (in a planar-aligned cell) leads to a display of the deformed helical ferroelectric mode. Dependence of the apparent tilt angle on the electric field does show that the phase under study is helical. The electro-optical response, in terms of the transmittance through the cell, as a function of the electric field can be explained by two competing mechanisms: the rotation around the long molecular axis and the rotation of the director (optical axis) around the cone. For higher fields, the chiral flipping is mostly the outcome, whereas the optical switching occurs by rotation on the cone for low fields. The chiral flipping also occurs at relatively higher temperatures, where the energy barrier to rotation of a molecule around its long molecular axis is significantly reduced. Results of the unwinding process of the helix by the electric field suggest that the structure of SmC$_S$P$_F^{hel}$ phase is similar to that of SmC$^*_\alpha$. In both cases, helix is formed because the structure provides an escape from the large macroscopic polarization and is presumably possible only in weakly tilted smectic phases. The only difference between SmC$^*_\alpha$ and SmCP$_\alpha$ appears to be that the former is formed by the molecules which are permanently chiral whereas the latter is formed by achiral molecules, but the achiral symmetry breaking should occur transiently or conformationally. It is suggested that due to a correspondence between the characteristics of two phases, theory of SmC$^*_\alpha$ should be applicable to SmCP$_\alpha$. The helical pitch in SmC$_S$P$_F^{hel}$ (SmCP$_\alpha$) is suggested to be incommensurate with an integral number of layer thickness as in SmC$^*_\alpha$. However, since SmCP$_\alpha$ phase is formed by achiral molecules, left- and right-handed helices are formed stochastically in opposite-handed domains. Also heliconical SmC$_{TB}$ phase is formed by achiral molecules (bent dimesogens) at the transition from the orthogonal to the tilted smectic phase, but the formation of this phase appears not to be related to the emergence of polarization [7].

Recently, incommensurate helical precession pitch has been determined using carbon-edge soft x-ray scattering technique of the compound **1/14** and is found to be 15 nm depending on the temperature [32] in line with the value obtained in our previous AFM investigation of **1/16** [1].

ACKNOWLEDGMENTS

Work of the Dublin group was partially funded by Science Foundation Ireland (IE), Grant No. 13/US/I2866, as part of the US–Ireland R and D Partnership program jointly administered with the U.S. NSF (Grant No. NSF-DMR-1410649) for which we also thank the Coordinator Prof. Satyendra Kumar. One of the authors (J.K.V.) acknowledges Prof. Jang-Kun Song of Sungkyunkwan University, Suwon, Korea and his group's kind hospitality during his visit to Korea in 2018. Discus-

sions with Atsuo Fukuda and Alexander V. Emelyanenko are acknowledged. The authors also acknowledge help of V. Swaminathan and V. P. Panov for making a schematic of Fig. 11. The support by the DFG (Ts 39/24-2) for the Halle group is acknowledged.

APPENDIX

List of Abbreviations:

Cry - crystalline solid state

Iso - isotropic liquid state

Sm*A*- uniaxial smectic LC phase with nontilted or tilt randomized organization of the molecules in the layers

SmAP_R- high-permittivity paraelectric Sm*A* phase

SmC - tilted smectic LC phase

SmC_S- SmC phase with uniform (synclinic) tilt in adjacent layers

SmC_A - SmC phase with opposite (anticlinic) tilt in adjacent layers

SmC_SP_R - high-permittivity paraelectric SmC_S phase

SmC_SP_A/SmC_AP_A synclinic SmC_S / anticlinic SmC_A antiferroelectric phase (polar layers with antipolar correlation)

SmC_SP_F - ferroelectric polar SmC_S phase (polar layers with synpolar correlation)

$SmC_SP_F^{hel}$ - uniaxial SmC_SP_F phase with heliconical superstructure and short incommensurate pitch (polar layers with an angle $> 0^\circ$ and $< 180^\circ$ ($\sim 120^\circ$ but not exactly 120°) between the polar directions of adjacent layers)

SmC^*_α - uniaxial heliconical SmC^* phase with short pitch exhibited by uniformly or scalemic chiral rodlike molecules; the asterisk indicates that the mesophase is formed by chiral molecules

Explanation of SmC_SP_X phase is given in Ref. [2].

$SmCP_\alpha$ - uniaxial heliconical SmC phase with short pitch helix with its axis perpendicular to the layer planes, exhibited by achiral molecules with spontaneous symmetry breaking of achirality; pitch of the helix is incommensurate with the layer periodicity

p_o -helical pitch

P_S spontaneous polarization

c_p - piezoelectric coefficient

c_f -flexoelectric coefficient

P_i- polarization of the *i*th layer.

g - molecular positional correlation factor in adjacent layers

$\Delta\varphi = \varphi_{i+1} - \varphi_i$; the $\boldsymbol{c}$-director twist-angle difference in between the adjacent layers

$\Delta \boldsymbol{n}_{i\pm1}$ is the vectorial difference in the nematic director in the $(i+1)$ and $(i-1)$ layers.

$\boldsymbol{M}_i$ is the complex order parameter of the *i*th layer.

POM - polarizing optical microscopy

[1] S. P. Sreenilayam, Yu. P. Panarin, J. K. Vij, V. P. Panov, A. Lehmann, M. Poppe, M. Prehm, and C. Tschierske, Spontaneous helix formation in non-chiral bent-core liquid crystals with fast linear-electro-optic effect, Nat. Commun. **7**, 11369 (2016).

[2] S. P. Sreenilayam, Yu. P. Panarin, J. K. Vij, A. Lehmann, P. Poppe, and C. Tschierske, Development of ferroelectricity in the smectic phases of 4-cyanoresorcinol derived achiral bent-core liquid crystals with long terminal alkyl chains, Phys. Rev. Mater. **1**, 035604 (2017).

[3] M. A. Alaasar, M. Prehm, M. Nagaraj, J. K. Vij, and C. Tschierske, A liquid crystalline phase with uniform tilt, local order and capability of symmetry breaking, Adv. Mater. **25**, 2186 (2013).

[4] D. Pociecha, M. Cepic, E. Gorecka, and J. Mieczkowski, Ferroelectric Mesophase with Randomized Interlayer Structure, Phys. Rev. Lett. **91**, 185501 (2003).

[5] Y. Shimbo, E. Gorecka, D. Pociecha, F. Araoka, M. Goto, Y. Takanishi, K. Ishikawa, J. Mieczkowski, K. Gomola, and H. Takezoe, Electric-Field Induced Polar Biaxial Order in a Non-Tilted Smectic Phase of an Asymmetric Bent-Core Liquid Crystal, Phys. Rev. Lett. **97**, 113901 (2006).

[6] Y. P. Panarin, M. Nagaraj, S. Sreenilayam, J. K. Vij, A. Lehmann, and C. Tschierske, Sequence of Four Orthogonal Smectic Phase in an Achiral Bent-Core Liquid Crystal: Evidence for the $SmAP_\alpha$ Phase, Phys. Rev. Lett. **107**, 247801 (2011).

[7] J. P. Abberley, R. Killah, R. Walker, J. M. D. Storey, C. T. Imrie, M. Salamonczyk, C. Zhu, E. Gorecka, and D. Pociecha, Heliconical smectic phase formed by achiral molecules, Nat. Commun. **9**, 228 (2018).

[8] A. Fukuda, Y. Takanishi, T. Isozaki, and H. Takezoe, Antiferroelectric smectic liquid crystals, J. Mater. Chem. **4**, 997 (1994).

[9] V. Borsch, Y.-K. Kim, J. Xiang, M. Gao, A. Jákli, V. P. Panov, J. K. Vij, C. T. Imrie, M. G. Tamba, G. H. Mehl, and O. D. Lavrentovich, Nematic twist bend phase with nanoscopic modulation of molecular orientation, Nat. Commun. **4**, 2635 (2013).

[10] S. P. Sreenilayam, V. P. Panov, J. K. Vij, and G. Shanker, The N_{TB} phase in an achiral asymmetrical bent-core liquid crystal terminated with symmetric alkyl chains, Liq. Cryst. **44**, 244 (2017).

[11] D. M. Agra-Koojiman, G. Singh, M. R. Fisch, M. R. Vengatesan, J.-K. Song, and S. Kumar, The oblique chiral nematic phase in calamitic bimesogens, Liq. Cryst. **44**, 191 (2017).

[12] K. Merkel, A. Kocot, J. K. Vij, and G. Shanker, Distortions in structures of the twist bend nematic phase of a bent-core liquid crystal by the electric field, Phys. Rev. E **98**, 022704 (2018).

[13] G. Pajak, L. Longa, and A. Chrzanowska, Nematic twist-bend in an external field, Proc. Natl. Acad. Sci. USA **115**, E10303 (2018).

[14] C. Meyer, Nematic twist-bend phase under external constraints, Liq. Cryst. **43**, 2144 (2016).

[15] Yu. P. Panarin, S. P. Sreenilayam, J. K. Vij, A. Lehmann, and C. Tschierske, A fast linear electro-optical effect in a non-chiral bent core liquid crystal, J. Mater. Chem. C **5**, 12585 (2017).

[16] N. A. Clark and S. T. Lagerwall, Submicrosecond bistable electro-optic switching in liquid crystals, Appl. Phys. Lett. **36**, 899 (1980).

[17] E. P. Pozhidaev, A. D. Kiselev, A. K. Srivastava, V. G. Chigrinov, H.-S. Kwok, and M. V. Minchenko, Optical Kerr

effect and phase modulation of light in deformed-helix ferroelectric liquid crystals with subwavelength pitch, Phys. Rev. E **87**, 052502 (2013).

[18] J.-K. Song, J. K. Vij, and B. K. Sadashiva, Conoscopy of chiral smectic liquid crystal cells, J. Opt. Soc. Am. A **25**, 1820 (2008).

[19] M. Alaasar, M. Prehm, M. Poppe, M. Nagaraj, J. K. Vij, and C. Tschierske, Development of polar order and tilt in lamellar liquid crystalline phases of a bent-core mesogen, Soft Matter **10**, 5003 (2014); M. Alaasar, M. Prehm, M.-G. Tamba, N. Sebastián, A. Eremin, and C. Tschierske, Development of polar order in the liquid crystal phases of a 4-cyanoresorcinol-based bent-core mesogen with fluorinated azobenzene wings, ChemPhysChem **17**, 278 (2016).

[20] V. P. Panov, M. Nagaraj, J. K. Vij, Yu. P. Panarin, A. Kohlmeier, M. G. Tamba, R. A. Lewis, and G. H. Mehl, Spontaneous Periodic Deformations in Nonchiral Planar Aligned Bimesogens with a Nematic-Nematic Transition and a Negative Elastic Constant, Phys. Rev. Lett. **105**, 167801 (2010); R. Balachandran, V. P. Panov, J. K. Vij, A. Kocot, M. G. Tamba, R. Kohlmeir, and G. H. Mehl, Elastic properties of bimesogenic liquid crystals, Liq. Cryst. **40**, 681 (2013).

[21] C. Tschierske and G. Ungar, Mirror symmetry breaking by chirality synchronization in liquids and liquid crystals of achiral molecules, ChemPhysChem. **17**, 9 (2016).

[22] S. A. Pikin and V. L. Indenbom, Piezoeffects and ferroelectric phenomena in smectic liquid crystals, Ferroelectrics **20**, 151 (1978).

[23] L. A. Beresnev, V. G. Chigrinov, D. I. Dergachev, E. P. Poshidaev, J. Fünfschilling, and M. Schadt, Deformed helix ferroelectric liquid crystal display: A new electro-optic mode in ferroelectric chiral smectic C liquid crystals, Liq. Cryst. **5**, 1171 (1989).

[24] M. Nakata, R.-F. Shao, J. E. Maclennan, W. Weissflog, and N. A. Clark, Electric-Field-Induced Chirality Flipping in Smectic Liquid Crystals: The Role of Anisotropic Viscosity, Phys. Rev. Lett. **96**, 067802 (2006).

[25] S. Sreenilayam, Y. P. Panarin, J. K. Vij, M. Osipov, A. Lehmann, and C. Tschierske, Biaxial order parameter in the homologous series of orthogonal bent-core smectic liquid crystals, Phys. Rev E **88**, 012504 (2013).

[26] A. V. Emelyanenko and M. A. Osipov, Theoretical model for the discrete flexoelectric effect and a description for the sequence of intermediate smectic phases with increasing periodicity, Phys. Rev E **68**, 051703 (2003).

[27] R. Balachandran, V. P. Panov, Y. P. Panarin, J. K. Vij, M. G. Tamba, G. H. Mehl, and J. K. Song, Flexoelectric behaviour of bimesogenic liquid crystals in the nematic phase – Observation of a new self-assembly pattern at the twist-bend nematic and the nematic interface, J. Mater. Chem. C **2**, 8179 (2014).

[28] N. M. Shtykov, A. D. L. Chandani, A. V. Emelyanenko, A. Fukuda, and J. K. Vij, Two kinds of smectic-C^*_α subphases in a liquid crystal and their relative stability dependent on enantiomeric excess as elucidated by electric-field-induced birefringence experiment, Phys. Rev. E **71**, 021711 (2005).

[29] A. D. L. Chandani, N. M. Shtykov, V. P. Panov, A. V. Emelyanenko, A. Fukuda, and J. K. Vij, Discrete flexoelectric polarizations and biaxial subphases with periodicities other than three and four layers in chiral smectic liquid crystals frustrated between ferroelectricity and antiferroelectricity, Phys. Rev. E **72**, 041705 (2005).

[30] K. L. Sandhya, J. K. Vij, A. Fukuda, and A. V. Emelyanenko, Degeneracy lifting near the frustration points due to long-range interlayer interaction forces and the resulting varieties of polar chiral tilted smectic phases, Liq. Cryst. **36**, 1101 (2009).

[31] V. P. Panov, B. K. McCoy, Z. Q. Liu, J. K. Vij, J. W. Goodby, and C. C. Huang, Investigations of nanoscale helical pitch in smectic-C^*_α and smectic-C^* phases of a chiral smectic liquid crystal using differential optical reflectivity measurements, Phys. Rev. E **74**, 011701 (2006).

[32] A. A. S. Green, M. R. Tuchband, R. Shao, Y. Shen, R. Visvanathan, A. E. Duncan, A. Lehmann, C. Tschierske, E. D. Carlson, E. Guzman, M. Kolber, D. M. Walba, C. S. Park, M. A. Glaser, J. E. Maclennan, and N. A. Clark, Chiral Incommensurate Helical Phase in a Smectic of Achiral Bent-Core Mesogens, Phys. Rev. Lett. **122**, 107801 (2019).

Correction: Minor errors in Eqs. (4) and (14) have been fixed.